JOURNAL OF AGRICULTURAL AND FOOD CHEMISTRY

Article

pubs.acs.org/JAFC

Bitter Taste Receptor Activation by Flavonoids and Isoflavonoids: Modeled Structural Requirements for Activation of hTAS2R14 and hTAS2R39

Wibke S. U. Roland,[†] Leo van Buren,[§] Harry Gruppen,[†] Marianne Driesse,[†] Robin J. Gouka,[§] Gerrit Smit,[†,#] and Jean-Paul Vincken*,[†]

[†]Laboratory of Food Chemistry, Wageningen University, 6708 WG Wageningen, The Netherlands

[§]Unilever R&D, 3133 AT Vlaardingen, The Netherlands

Supporting Information

ABSTRACT: Many flavonoids and isoflavonoids have an undesirable bitter taste, which hampers their use as food bioactives. The aim of this study was to investigate the effect of a large set of structurally similar (iso)flavonoids on the activation of bitter receptors hTAS2R14 and hTAS2R39 and to predict their structural requirements to activate these receptors. In total, 68 compounds activated hTAS2R14 and 70 compounds activated hTAS2R39, among which 58 ligands were overlapping. Their activation threshold values varied over a range of 3 log units between 0.12 and 500 μM. Ligand-based 2D-fingerprint and 3D-pharmacophore models were created to detect structure−activity relationships. The 2D models demonstrated excellent predictive power in identifying bitter (iso)flavonoids and discrimination from inactive ones. The structural characteristics for an (iso)flavonoid to activate hTAS2R14 (or hTAS2R39) were determined by 3D-pharmacophore models to be composed of two (or three) hydrogen bond donor sites, one hydrogen bond acceptor site, and two aromatic ring structures, of which one had to be hydrophobic. The additional hydrogen bond donor feature for hTAS2R39 ligands indicated the possible presence of another complementary acceptor site in the binding pocket, compared to hTAS2R14. Hydrophobic interaction of the aromatic feature with the binding site might be of higher importance in hTAS2R14 than in hTAS2R39. Together, this might explain why OH-rich compounds showed different behaviors on the two bitter receptors. The combination of in vitro data and different in silico methods created a good insight in activation of hTAS2R14 and hTAS2R39 by (iso)flavonoids and provided a powerful tool in the prediction of their potential bitterness. By understanding the "bitter motif", introduction of bitter taste in functional foods enriched in (iso)flavonoid bioactives might be avoided.

KEYWORDS: *bitterness, T2R, TAS2R, hTAS2R, flavonoids, pharmacophore, modeling*

INTRODUCTION

Phenolic compounds, such as flavonoids and isoflavonoids, are the focus of health research. Isoflavonoids mainly occurring in legumes, such as soybeans, have been associated with prevention of some cancers, cardiovascular disease, menopausal complaints, and osteoporosis.[1] Flavonoids occur in many different plants and are widely present in our diet. Among others, they might play a role in the reduced incidence of cancer and cardiovascular diseases.[2,3] Unfortunately, many (iso)flavonoids have a negative impact on sensory perception as they can taste bitter.[4] The bitter taste of soybean isoflavones has been described in several sensory studies.[5,6] Recently, we showed that several soybean isoflavones activated the human bitter taste receptors hTAS2R14 and hTAS2R39 and partially elucidated the isoflavonoid substitution pattern favorable for activation of both receptors.[7]

Bitter taste receptor hTAS2R14 is known to be activated by a large number of compounds originating from different chemical classes.[7−13] For hTAS2R39, on the other hand, a rather moderate number of agonists have been reported,[7,9,14−17] and this receptor seemed to be less broadly tuned than hTAS2R14.[9] Recently, hTAS2R39 has been reported to be activated by tea catechins,[14] which belong to the group of flavonoids.

There are also numerous flavonoids that do not traditionally occur in our diet and for which the taste is often not known. It is hypothesized that the bitter taste characteristics can be predicted once the molecular signatures of (iso)flavonoids for activation of hTAS2R14 and hTAS2R39 are known. Originating in pharmaceutical science, the concept of molecular modeling gains importance in food science[18] and might be employed in facilitating such predictions. A 2D-fingerprint model is based on a binary representation of a molecule in which each bit indicates the presence or absence of a molecular fragment.[19] A 3D-pharmacophore model operates with a set of features together with their relative spatial orientation, which relates to a set of chemical features in a molecule. These features are recognized by amino acid residues in the receptor binding site with complementary functions, ultimately explaining that molecule's biological activity.[20,21] Recently, Ley et al.[22] described a pharmacophore model that, on docking in a hTAS2R10 structural model, allowed identification of a masking agent for the bitter taste of caffeine. Furthermore,

Received: July 31, 2013
Revised: October 5, 2013
Accepted: October 11, 2013
Published: October 11, 2013

ligand-based pharmacophore modeling has been applied to understand structure−activity relationships of odors[23] and to explain interactions between flavor compounds and β-lactoglobulin.[24]

The objective of the present study was to study the behavior of flavonoids toward activation of hTAS2R14 and hTAS2R39. Their activation would indicate that the compounds tested have a bitter taste. To this end, a large subset of flavonoids, or flavonoid analogues, were tested, and the threshold and EC_{50} values of the active compounds were determined. A second objective was to investigate the chemical space of flavonoids, and isoflavonoids, in relation to the activation of bitter receptors hTAS2R14 and hTAS2R39. By linking the receptor activation with the compound's molecular structure, 2D-fingerprint models and ligand-based 3D-pharmacophore models for each of the two bitter receptors were established. These models map the structural requirements for ligands with an isoflavonoid, flavonoid, or similar structure for these two receptors. Altogether, they distinguish active from inactive (iso)flavonoids and enable predicting bitterness of similar compounds with unknown taste properties.

MATERIALS AND METHODS

Receptor Assays. *Materials.* Compounds tested were purchased from Indofine Chemical Co. (Hillsborough, NJ, USA), Extrasynthese (Genay, France), Sigma-Aldrich (Steinheim, Germany), Brunschwig (Amsterdam, The Netherlands), Bioconnect (Huissen, The Netherlands), or WAKO (Neuss, Germany). The majority of compounds were ≥99% (18 compounds), ≥98% (44 compounds), or ≥97% (15 compounds) pure. Compounds **38** and **71** were ≥96% pure; **22**, **39**, **43**, **45**, **50**, **51**, **59**, **70**, **78**, and **94** were ≥95% pure; **33**, **54**, **56**, **74**, **79**, **80**, and **88** were ≥90% pure; and **37** was ≥85% pure. Each compound was dissolved in DMSO (Sigma-Aldrich) to a 100 mM stock concentration. Trypan blue solution (0.4% w/v) was purchased from Sigma-Aldrich.

Tyrode's buffer (140 mM NaCl, 5 mM KCl, 10 mM glucose, 1 mM $MgCl_2$, 1 mM $CaCl_2$, and 20 mM Hepes, pH 7.4) with 0.5 mM probenecid (Sigma-Aldrich) was used for dilution of compound−DMSO stock solutions and for calcium imaging assays. All compounds were tested for autofluorescence and toxic effects on the cells used at a concentration of 1 mM as described before,[7] without observed abnormalities.

In Vitro Assessment of hTAS2R14 and hTAS2R39 Activation by Intracellular Calcium Release. Activation of bitter taste receptors expressed in HEK293 cells leads to release of intracellular Ca^{2+}.[25] This was measured using the fluorescent calcium dye Fluo-4-AM (2.5 μM, Molecular Probes, Eugene, OR, USA) in a FlexStation II 384 or FlexStation III (Molecular Devices Corp., Sunnyvale, CA, USA) for 90 s (excitation 485 nm/emission 520 nm). The expression of hTAS2R14 and hTAS2R39 in HEK293 cells, the maintenance of the cells, and the measuring procedure were performed as reported earlier.[7]

In total, a set of 97 compounds are described in this study, of which 19 isoflavonoids were reported in our earlier publication,[7] and 78 other compounds were tested additionally. Stock solutions of test compounds were prepared in DMSO and diluted to the appropriate concentration in Tyrode's buffer, not exceeding a DMSO concentration of 1% (v/v). Screening of hTAS2R14 and hTAS2R39 for activation was performed at 500 μM concentrations of test compounds. In case of activation, test compounds were measured at concentration ranges up to 1 mM to establish dose−response curves. Noninduced cells, not expressing the bitter receptors, were always measured in parallel to verify specificity of receptor activation. As positive controls for receptor activation, in each plate duplicate measurements with epicatechin gallate[14] for hTAS2R39 or with naphthoic acid[8] (or genistein) for hTAS2R14 were performed. All experiments were conducted in duplicate on two or more different days. Some compounds were not completely soluble at high concentrations and, therefore, their real potency might be underestimated.

Calcium Assay Data Processing and Statistical Analysis. Data processing and statistical analysis were done as reported previously.[7] SoftMax Pro 5.4 software (Molecular Devices Corp.) was used to plot the fluorescence signals. The fluorescence value ($\Delta F/F_0$), representing receptor activity, was calculated by subtracting the baseline fluorescence (F_0) prior to loading from the maximum fluorescence (F) after addition of the bitter compounds, divided by the signal of the baseline to normalize background fluorescence.[26] Besides the response of induced cells, also the response of noninduced cells (not expressing the bitter receptor) was measured as negative control for every compound at every concentration on the same plate. In cases that a nonspecific signal occurred, the respective compound was considered as active when the signal of the induced cells was significantly higher than that of the negative control cells ($P = 0.05$). The signal intensity of noninduced cells was taken at the reading point at which the signal of the induced cells was maximal. Threshold values of the agonists toward receptor activation were determined as first concentration showing significant difference to the baseline and to the response of noninduced cells. Differences were considered to be significant at $P < 0.05$, using a t test (two-sided, nonpaired) (SAS 9.2, Sas Institute Inc., Cary, NC, USA). Dose−response curves were established as nonlinear regression curves using Graph Pad Prism (version 4 for Windows, Graph Pad Software, San Diego, CA, USA). The error bars reflect the standard error of the mean (SEM). EC_{50} values were calculated for compounds that reached a maximum in the dose−response curve (after subtraction of the response of noninduced cells, if applicable). For compounds that evoked high nonspecific signals at higher concentrations, only the data for the appropriate concentrations are shown in the figures.

Modeling. *2D-Fingerprint Modeling.* 2D modeling was performed using Pipeline Pilot v8.0, (Accelrys, San Diego, CA, USA). The chemical structures of the 97 compounds tested were derived from the SMILES (simplified molecular-input line-entry system) notations (Supporting Information S1). Results at the screening concentration of 500 μM were used. Compounds showing ambiguous results (22 compounds for hTAS2R14; 21 compounds for hTAS2R39) were excluded. This resulted in 75 and 76 compounds suitable for modeling of receptor activation of hTAS2R14 and hTAS2R39, respectively. The majority of these compounds were used for model building (training set), containing both active and inactive compounds, whereas ∼10% of the structurally most diverse compounds were excluded from model building for validation purposes (test set).

The optimal fingerprint model was obtained by building numerous models based on different fingerprint types. This optimization was done with the training set, using the Bayesian interference method and leave-one-out settings.[19,27] Three-fold cross-validations were performed to evaluate the models, in which ranking of the best models was primarily based on the receiver operating characteristic (ROC) scores (see Supporting Information S2−S4). The highest ranking models were further validated by the test sets, resulting in the final model selection. ECFP-10 and ECFP-8 fingerprint models were selected for hTAS2R14 and hTAS2R39, respectively. Their ROC scores were close to 1, which indicated excellent accuracy. Extended-connectivity fingerprints (ECFP) use charge and hybridization of the atom (extended (E)) and connectivity (C)) and return a list of fragments present in the molecule,[19] of which in this case the maximum diameters of a fragment were 10 and 8 bond lengths, respectively.

For identification of key molecular features for bitter receptor activation, 20 "good" (G) and 20 "bad" (B) fingerprint fragments were calculated for each model. Each of them has a Bayesian score. If this score is positive, the likelihood that the fragment is a member of the active subset increases and vice versa. A selection of four illustrative fragments is shown under Results; the full list is specified in the Supporting Information (S5−S9).

3D-Pharmacophore Modeling. 3D-pharmacophore modeling was performed using Discovery Studio v3.1 (Accelrys). In contrast to 2D-fingerprint modeling, a training set for 3D-pharmacophore modeling is

based on only a few highly active compounds. The selection for pharmacophore training ligands on bitter receptor activation was based on activation thresholds, as EC_{50} values were not available for all (iso)flavonoids. Compounds were categorized by their threshold values into highly active (threshold $\leq$ 32 μM), moderately active (threshold > 32−500 μM), and inactive compounds (not active up to 500 μM) (Table 2). Twenty-four compounds for hTAS2R14 and 20 compounds for hTAS2R39 showed ambiguous results or high nonspecific signals and were excluded from modeling. Besides low threshold, the training ligands had to be diverse in backbone structure and substitution pattern. Seven highly active compounds were chosen as training ligands for each receptor (Table 1). One of the training ligands selected for building the hTAS2R39 pharmacophore was an anthocyanidin and required special attention. Due to the pH dependence of the anthocyanidin structure (shifting equilibria between flavylium cation structure, quinoid tautomers, hemiketal, and chalcone),[28,29] multiple forms were included for modeling.

Training compounds were subjected to internal strain energy minimization and conformational analysis (maximum number of conformers = 200; generation type, best quality; energy range = 10 kcal/mol above the calculated global minimum). Using the hiphop and hiphop refine algorithms of Discovery Studio, the chemical features optimized for exploring the spatial pharmacophore map of this group of compounds were "hydrogen bond acceptor", "hydrogen bond donor", "hydrophobic aromatic", "hydrophobic aliphatic", and "ring aromatic". The "hydrophobic aromatic" feature describes an aromatic ring that is hydrophobic, the spatial orientation of which is irrelevant. The "ring aromatic" feature describes an aromatic ring that can be hydrophobic or hydrophilic, depending on its substitutions. Furthermore, the plane of this aromatic ring has a fixed orientation toward the receptor binding site. The pharmacophore models were trained with qualitative data, and thus the features are not weighed, and the relevance of each feature was considered as equal. The quality of mapping is described by fit values. A feature that maps exactly on the respective atom has a fit value of 1, and a feature that does not map has a fit value of 0. The fit values and relative energies of all compounds are summarized in Supporting Information S1. Mapping is done by rotation and translation of the molecule to optimize the superimposition of the molecule on the features; meanwhile, additionally the torsion angles are altered whereby the maximal relative energy should not exceed 10 kcal/mol, compared to its optimal energetic state of 0 kcal/mol.

The pharmacophore protocol created 10 hypotheses for each run. These hypotheses were analyzed to find the optimal model. Hypotheses were scored on the basis of the confusion matrix table, ROC plots, rank score, direct hit/partial hit, and maximal fit value (additional information given in Supporting Information S10−S14). The optimization involved variation of features and/or locations to optimize sensitivity and specificity of the structure-based activity prediction.

Pharmacophore building for ligands of hTAS2R14 resulted in a five-feature pharmacophore, whereas for ligands of hTAS2R39, it resulted in a six-feature pharmacophore. In the case of the model built for hTAS2R14, a ligand had to map all five features to be predicted as active, whereas in the case of the model built for hTAS2R39, ligands were allowed to map five of six features, without disqualifying them as active. Quality of mapping and correctness of predictions were analyzed with a heat map (Supporting Information S15−S16).

RESULTS

Compound Selection and Qualitative Screening for hTAS2R Activation. Ninety-seven compounds were screened for activation of bitter receptors hTAS2R14 and hTAS2R39, on the basis of variation in backbone structure and their substitution pattern (Table 1). One example is shown in Figure 1A. 6,7-Dimethoxyflavone (**11**) clearly activated hTAS2R14, whereas it did not activate hTAS2R39. All test compounds were categorized as "+", "−", and "±", depending on their extent of receptor activation. The latter designation was given when results were ambiguous even after three repetitions in duplicate. In vitro results identified 60 compounds that activated hTAS2R14 and 67 compounds that activated hTAS2R39 at the screening concentration of 500 μM. In contrast, 15 compounds did not activate hTAS2R14, whereas 9 compounds did not activate hTAS2R39. The remaining compounds could not be unambiguously classified at the screening concentration (Table 1).

Dose−Response Behavior of Selected (Iso)flavonoids on hTAS2R14 and hTAS2R39. All (iso)flavonoids (or similar) that activated one or both of the two bitter receptors at the screening concentration were measured at different concentrations to establish dose−response curves, the threshold and EC_{50} values of which are summarized in Table 1. Their threshold values varied over a range of 3 log units between 0.12 and 500 μM. Although many compounds activated both bitter receptors, the threshold concentrations for each individual receptor sometimes varied. For example, resveratrol (**95**) (Figure 1B) had a threshold value with hTAS2R14 of 16 μM and an EC_{50} value of 30.3 μM, whereas with hTAS2R39 these were 63 and 109 μM, respectively. An even larger difference in bitter receptor activation was observed for epigallocatechin gallate (**59**) (Figure 1C), with a threshold of 32 μM and an EC_{50} of 161 μM for hTAS2R39 and a threshold of 250 μM for hTAS2R14. The EC_{50} value for hTAS2R14 could not be calculated. Other compounds showed almost identical behavior toward both bitter receptors. For example, scutellarein (**23**; Figure 1D) activated both receptors from 8 μM onward with EC_{50} values of 35.0 and 40.3 μM for hTAS2R14 and hTAS2R39, respectively.

Influence of Small Structural Changes on Bitter Receptor Activation. Small structural changes had different effects on receptor activation. A few examples for hTAS2R39 are shown in Figure 2. Phloretin (**70**) and naringenin (**50**) have the same A- and B-ring substitutions, but differ in an open and closed C-ring, respectively (Figure 2A). Nevertheless, both compounds have the same threshold of 8 μM and differ only slightly in EC_{50} values (41.3 μM for **70** and 32.9 μM for **50**). In this case, the change of the C-ring structure had a small effect. In contrast, eriodictyolchalcone (**65**) and luteolin (**20**), differing similarly in C-ring configuration, showed different behaviors in receptor activation (Figure 2B). The thresholds were 16 μM for **65** and 0.5 μM for **20**, whereas the EC_{50} values were 55.5 μM for **65** and 7.3 μM for **20**.

In some cases, similar effects were observed for variation in the B-ring structure. For example, the structural difference between eriodictyol (**43**) and homoeriodictyol (**46**) did not affect receptor activation (Figure 2C). For other compounds, a change in B-ring substituents had an effect, for example, comparing luteolin (**20**) (two OH-groups on the B-ring, highly active) to tricetin (**24**) (three OH-groups on the B-ring, threshold = 250 μM, curve not shown). Figure 2D compares three flavones that vary in A-ring substitution, 3′,4′,7-trihydroxyflavone (**27**), 6-methoxyluteolin (**22**), and luteolin (**20**), with effects on threshold (16, 8, and 0.5 μM, respectively) and EC_{50} values (141, 22.9, and 7.3 μM, respectively).

There was no obvious universal relationship between structural denominator and activity. Considering the large number of compounds tested, modeling was employed to detect structure−activity relationships.

2D-Fingerprint Modeling. The best separation between active and inactive compounds was achieved by the ECFP-10

Table 1. Chemical Structures of Compounds Tested and Their Behavior on hTAS2R14 and hTAS2R39 Concerning Activity, Threshold, and EC_{50} Values[a]

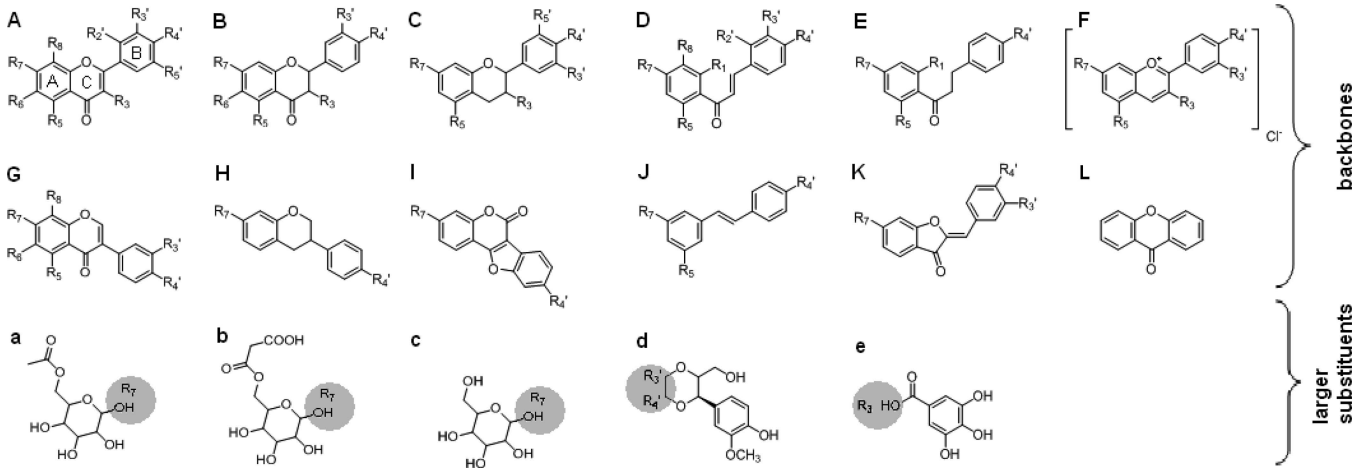

compound	no.	activity hTAS2R 14	activity hTAS2R 39	threshold hTAS2R 14	threshold hTAS2R 39	EC_{50} hTAS2R 14	EC_{50} hTAS2R 39	backbone	R_1	R_3	R_5	R_6	R_7	R_8	$R_{2'}$	$R_{3'}$	$R_{4'}$	$R_{5'}$
flavones																		
acacetin	**1**	−	±	na	nsp	nd	nd	A		H	OH	H	OH	H	H	H	OCH_3	H
apigenin	**2**	+	+	8	1	nd	nd	A		H	OH	H	OH	H	H	H	OH	H
chrysin	**3**	+	+	63	16	nd	nd	A		H	OH	H	OH	H	H	H	H	H
chrysoeriol	**4**	+	±	500	na	nd	nd	A		H	OH	H	OH	H	H	OCH_3	OH	H
5,2′-dihydroxyflavone	**5**	−	+	na	500	nd	nd	A		H	OH	H	H	H	OH	H	H	H
5,3′-dihydroxyflavone	**6**	±	±	na	na	nd	nd	A		H	OH	H	H	H	H	OH	H	H
5,4′-dihydroxyflavone	**7**	+	+	250	500	nd	nd	A		H	OH	H	H	H	H	H	OH	H
6,4′-dihydroxyflavone	**8**	+	+	125	500	nd	nd	A		H	H	OH	H	H	H	H	OH	H
7,4′-dihydroxyflavone	**9**	+	+	16	125	nd	nd	A		H	H	H	OH	H	H	H	OH	H
5,7-dimethoxyflavone[e]	**10**	+	+	16	32	nd	nd	A		H	OCH_3	H	OCH_3	H	H	H	H	H
6,7-dimethoxyflavone	**11**	+	−	125	na	nd	nd	A		H	H	OCH_3	OCH_3	H	H	H	H	H
flavone	**12**	+	+	8	8	20.5	45.9	A		H	H	H	H	H	H	H	H	H
gardenin A	**13**	−	±	na	na	nd	nd	A		H	OH	OCH_3	OCH_3	OCH_3	H	OCH_3	OCH_3	OCH_3
genkwanin	**14**	−	+	na	500	nd	nd	A		H	OH	H	OCH_3	H	H	H	OH	H
5-hydroxyflavone	**15**	±	+	na	500	nd	nd	A		H	OH	H	H	H	H	H	H	H
4′-hydroxyflavone	**16**	±	+	na	500	nd	nd	A		H	H	H	H	H	H	H	OH	H
5-hydroxy-3′-methoxyflavone	**17**	−	−	na	na	nd	nd	A		H	OH	H	H	H	H	OCH_3	H	H
4′-hydroxy-6-methoxyflavone	**18**	+	−	125	na	nd	nd	A		H	H	OCH_3	H	H	H	H	OH	H
4′-hydroxy-7-methoxyflavone	**19**	+	+	250	250	nd	nd	A		H	H	H	OCH_3	H	H	H	OH	H
luteolin	**20**	+	+	2	0.5	6.0	7.3	A		H	OH	H	OH	H	H	OH	OH	H
6-methoxyflavone	**21**	±	−	na	na	nd	nd	A		H	H	OCH_3	H	H	H	H	H	H
6-methoxyluteolin[b]	**22**	+	+	4	8	11.0	22.9	A		H	OH	OCH_3	OH	H	H	OH	OH	H
scutellarein[b,c]	**23**	+	+	8	8	35.0	40.3	A		H	OH	OH	OH	H	H	H	OH	H

dx.doi.org/10.1021/jf403387p | J. Agric. Food Chem. 2013, 61, 10454−10466

Table 1. continued

compound	no.	activity hTAS2R 14	activity hTAS2R 39	threshold hTAS2R 14	threshold hTAS2R 39	EC_{50} hTAS2R 14	EC_{50} hTAS2R 39	backbone	R_1	R_3	R_5	R_6	R_7	R_8	$R_{2'}$	$R_{3'}$	$R_{4'}$	$R_{5'}$
tricetin	**24**	±	+	na	250	nd	nd	A		H	OH	H	OH	H	H	OH	OH	OH
5,7,2′-trihydroxyflavone	**25**	+	+	8	4	21.1	35.3	A		H	OH	H	OH	H	OH	H	H	H
5,3′,4′-trihydroxyflavone	**26**	±	±	na	nsp	nd	nd	A		H	OH	H	H	H	H	OH	OH	H
7,3′,4′-trihydroxyflavone	**27**	+	+	16	16	67.3	141	A		H	H	H	OH	H	H	OH	OH	H
5,7,4′-trimethoxyflavone	**28**	+	±	250	na	nd	nd	A		H	OCH_3	H	OCH_3	H	H	H	OCH_3	H
flavonols																		
datiscetin[b]	**29**	+	+	2	16	10.0	41.6	A		OH	OH	H	OH	H	OH	H	H	H
fisetin	**30**	±	+	nsp	1	nd	nd	A		OH	H	H	OH	H	H	OH	OH	H
flavonol	**31**	±	±	na	na	nd	nd	A		OH	H	H	H	H	H	H	H	H
gossypetin[d]	**32**	−	+	na	250	nd	388	A		OH	OH	H	OH	OH	H	OH	OH	H
herbacetin	**33**	+	+	125	125	nd	nd	A		OH	OH	H	OH	OH	H	H	OH	H
isorhamnetin	**34**	+	+	125	0.12	nd	nd	A		OH	OH	H	OH	H	H	OCH_3	OH	H
kaempferol	**35**	+	+	8	0.5	nd	nd	A		OH	OH	H	OH	H	H	H	OH	H
6-methoxyflavonol	**36**	−	±	na	nsp	nd	nd	A		OH	H	OCH_3	H	H	H	H	H	H
morin	**37**	+	+	8	2	nd	nd	A		OH	OH	H	OH	H	OH	H	OH	H
myricetin[d]	**38**	+	+	250	1	nd	nd	A		OH	OH	H	OH	H	H	OH	OH	OH
quercetagetin	**39**	±	+	250	2	nd	nd	A		OH	OH	OH	OH	H	H	OH	OH	H
quercetin	**40**	±	±	nsp	nsp	nd	nd	A		OH	OH	H	OH	H	H	OH	OH	H
3,6,3′,4′-tetrahydroxyflavone	**41**	±	+	8	2	nd	nd	A		OH	H	OH	H	H	H	OH	OH	H
3,7,4′-trihydroxyflavone	**42**	+	+	1	0.5	nd	nd	A		OH	H	H	OH	H	H	H	OH	H
flavanones																		
eriodictyol[b]	**43**	+	+	32	16	61.4	62.0	B		H	OH	H	OH			OH	OH	
flavanone	**44**	+	±	32	na	nd	nd	B		H	H	H	H			H	H	
hesperitin	**45**	±	±	16	8	nd	nd	B		H	OH	H	OH			OH	OCH_3	
homoeriodictyol[c]	**46**	+	+	32	32	63.9	84.9	B		H	OH	H	OH			OCH_3	OH	
4′-hydroxyflavanone[d]	**47**	−	±	na	na	nd	nd	B		H	H	H	H			H	OH	
liquiritigenin	**48**	+	+	32	16	59.2	64.5	B		H	H	H	OH			H	OH	
6-methoxyflavanone	**49**	±	−	na	na	nd	nd	B		H	H	OCH_3	H			H	H	
naringenin	**50**	+	+	16	8	36.2	32.9	B		H	OH	H	OH			H	OH	
pinocembrin	**51**	+	+	8	4	39.1	48.9	B		H	OH	H	OH			H	H	
flavanonols																		
fustin	**52**	+	+	500	250	nd	nd	B		OH	H	H	OH			OH	OH	
silibinin[d]	**53**	+	+	8	8	56.1	99.2	B, d		OH	OH	H	OH			d	d	
(+)-taxifolin	**54**	+	+	63	125	nd	nd	B		OH	OH	H	OH			OH	OH	
flavanols																		
(+)-catechin[d]	**55**	+	+	500	250	nd	nd	C		OH	OH		OH			OH	OH	H
(−)-epicatechin (EC)	**56**	±	+	500	250	nd	nd	C		OH	OH		OH			OH	OH	H
(−)-epicatechin gallate (ECG)	**57**	+	+	125	32	nd	151	C, e		e	OH		OH			OH	OH	H
(−)-epigallocatechin[e] (EGC)	**58**	−	+	na	500	nd	nd	C		OH	OH		OH			OH	OH	OH
(−)-epigallocatechin gallate[c] (EGCG)	**59**	+	+	250	32	nd	161	C, e		e	OH		OH			OH	OH	OH
chalcones[f]																		

dx.doi.org/10.1021/jf403387p | J. Agric. Food Chem. 2013, 61, 10454−10466

Table 1. continued

compound	no.	activity hTAS2R 14	activity hTAS2R 39	threshold hTAS2R 14	threshold hTAS2R 39	EC_{50} hTAS2R 14	EC_{50} hTAS2R 39	backbone	R_1	R_3	R_5	R_6	R_7	R_8	$R_{2'}$	$R_{3'}$	$R_{4'}$	$R_{5'}$
butein	**60**	+	+	16	125	nd	nd	D	H		OH		OH	H	H	OH	OH	
chalcone	**61**	+	±	32	na	nd	nd	D	H		H		H	H	H	H	H	
3,2′-dihydroxychalcone	**62**	±	+	8	8	24.5	53.6	D	H		OH		H	H	H	OH	H	
4,2′-dihydroxychalcone	**63**	±	±	na	na	nd	nd	D	H		OH		H	H	H	H	OH	
2′,4′-dihydroxychalcone	**64**	±	±	nsp	nsp	nd	nd	D	H		OH		OH	H	H	H	H	
eriodictyolchalcone[c]	**65**	+	+	32	16	40.7	55.5	D	OH		OH		OH	H	H	OH	OH	
4′-hydroxychalcone	**66**	±	±	16	nsp	nd	nd	D	H		H		OH	H	H	H	H	
isoliquiritigenin	**67**	±	±	16	16	nd	nd	D	H		OH		OH	H	H	H	OH	
2,2′,4′-trihydroxychalcone	**68**	+	+	8	2	nd	nd	D	H		OH		OH	H	OH	H	H	
4,2′,5′-trihydroxychalcone[e]	**69**	+	+	125	2	nd	nd	D	H		OH		H	OH	H	H	OH	
dihydrochalcones[f]																		
phloretin[b]	**70**	+	+	16	8	30.2	41.3	E	OH		OH		OH	H	H	H	OH	
anthocyanidins																		
cyanidin chloride[c]	**71**	+	+	250	32	nd	187	F		OH	OH		OH			OH	OH	
pelargoninidin chloride	**72**	+	+	63	32	nd	nd	F		OH	OH		OH			H	OH	
deoxyanthocyanidins																		
apigeninidin chloride[e]	**73**	−	−	na	na	nd	nd	F		H	OH		OH			H	OH	
isoflavones																		
acetylgenistin[c,d,e,g]	**74**	−	+	na	125	nd	nd	G, a			OH	H	a	H		H	OH	
biochanin A[g]	**75**	+	+	63	500	nd	nd	G			OH	H	OH	H		OH	OCH_3	
daidzein[g]	**76**	+	+	500	500	nd	nd	G			H	H	OH	H		H	OH	
daidzin[g]	**77**	±	±	na	na	nd	nd	G, c			H	H	c	H		H	OH	
7,4′-dimethoxy-5-hydroxyisoflavone[e]	**78**	−	−	na	na	nd	nd	G			OH	H	OCH_3	H		H	OCH_3	
7,4′-dimethoxyisoflavone	**79**	+	−	500	na	nd	nd	G			H	H	OCH_3	H		H	OCH_3	
formomonetin[d,g]	**80**	+	+	500	500	nd	nd	G			H	H	OH	H		H	OCH_3	
genistein[b,c,g]	**81**	+	+	4	8	28.9	49.4	G			OH	H	OH	H		H	OH	
genistin[g]	**82**	−	+	na	500	nd	nd	G, c			OH	H	c	H		H	OH	
glycitein[g]	**83**	+	+	500	500	nd	nd	G			H	OCH_3	OH	H		H	OH	
glycitin[g]	**84**	−	+	na	500	nd	nd	G, c			H	OCH_3	c	H		H	OH	
7-hydroxyisoflavone[g]	**85**	+	+	32	250	nd	315	G			H	H	OH	H		H	H	
7-hydroxy-6-methoxyisoflavone[g]	**86**	±	±	nsp	nsp	nd	nd	G			H	OCH_3	OH	H		H	H	
isoflavone[e,g]	**87**	+	−	250	na	nd	nd	G			H	H	H	H		H	H	
malonylgenistin[g]	**88**	−	+	na	500	nd	nd	G, b			OH	H	b	H		H	OH	
prunetin[g]	**89**	+	±	16	nsp	nd	nd	G			OH	H	OCH_3	H		H	OH	
6,7,4′-trihydroxyisoflavone[g]	**90**	+	+	250	250	nd	nd	G			H	OH	OH	H		H	OH	
7,8,4′-trihydroxyisoflavone[g]	**91**	+	+	63	63	124	184	G			H	H	OH	OH		H	OH	
7,3′,4′-trihydroxyisoflavone[g]	**92**	+	+	250	250	nd	nd	G			H	H	OH	H		OH	OH	
isoflavans																		
equol[b,g]	**93**	±	±	8	32	47.2	55.8	H					OH				OH	
coumestans[f]																		
coumestrol[g]	**94**	+	+	250	250	nd	nd	I					OH				OH	

dx.doi.org/10.1021/jf403387p | J. Agric. Food Chem. 2013, 61, 10454−10466

Table 1. continued

compound	no.	activity hTAS2R 14	activity hTAS2R 39	threshold hTAS2R 14	threshold hTAS2R 39	EC_{50} hTAS2R 14	EC_{50} hTAS2R 39	backbone	R_1	R_3	R_5	R_6	R_7	R_8	$R_{2'}$	$R_{3'}$	$R_{4'}$	$R_{5'}$
stilbenes[f]																		
resveratrol	**95**	+	+	16	63	30.3	109	J			OH		OH				OH	
aurones[f]																		
sulfuretin[c]	**96**	+	+	16	16	21.5	48.0	K					OH			OH	OH	
xanthones																		
xanthone[e]	**97**	+	+	250	500	nd	nd	L										

[a]Activity was determined at 500 μM screening concentration (+, active; −, inactive; ±, results ambiguous). Backbones: A, flavone (R_3 = H)/flavonol (R_3 = OH); B, flavanone (R_3 = H)/flavanonol (R_3 = OH); C, flavan (R_3 = H)/flavanol (R_3 = OH); D, chalcone; E, dihydrochalcone; F, anthocyanidin (R_3 = OH)/deoxyanthocyanidin (R_3 = H); G, isoflavone; H, isoflavan; I, coumestan; J, stilbene; K, aurone; L, xanthone. Side groups: a, 6-*O*-acetylglucose; b, 6-*O*-malonylglucose; c, glucose; d, 4-((2*S*)-3-(hydroxymethyl)-1,4-dioxan-2-yl)-2-methoxyphenol; e, gallic acid. na, not active up to 500 μM; nd, not determined; nsp, not specific, activity could not be determined due to nonspecific signals in the noninduced cells. [b]Training set used for pharmacophore building of hTAS2R14. [c]Training set used for pharmacophore building of hTAS2R39. [d]Test set used for fingerprint model of hTAS2R14. [e]Test set used for fingerprint model of hTAS2R39. [f]To facilitate comparison of positions of substitutions with the majority of the flavonoids, the usually applied residue numbering for chalcones, coumestans, stilbenes, and aurones was adapted. [g]Published previously.[7]

and ECFP-8 fingerprint models for hTAS2R14 and hTAS2R39, respectively. Figure 3 displays the predictions for the complete set of training and test molecules used for modeling. The ECFP-10 model for hTAS2R14 agonists predicted 93% of all compounds correctly. Two compounds were falsely predicted as active, and three compounds were falsely predicted as inactive. The ECFP-8 model for hTAS2R39 agonists predicted 96% of all compounds correctly. One compound was falsely predicted as active and two compounds were falsely predicted as inactive.

To identify key molecular features involved in bitter receptor activation, "good" and "bad" fingerprint fragments were established (see Supporting Information S5−S9), of which a selection of four illustrative fragments is shown here for the hTAS2R14 model (Figure 4). On the basis of the fragments it was observed that the flavanones and isoflavones were likely to trigger hTAS2R14. Flavones could activate this receptor as well, but there were fragments within some flavones assigned to the "bad" fragments, implying that some flavones caused less or no activation. Methoxylation and glycosylation seemed to impair activation of this receptor. Receptor hTAS2R39 had a high probability of activation by flavanones and flavonols and showed a similar behavior toward flavones as compared to hTAS2R14. Methoxylation fragments were not beneficial for activation by isoflavonoids. Glycosylation was not an obvious bad feature for this receptor. The fingerprint fragments helped in understanding which molecular features were obviously favorable and unfavorable for receptor activation were, but it was not possible to develop a most common substructure.

In conclusion, the 2D models possessed excellent predictive value for identification of bitter (iso)flavonoids activating hTAS2R14 or hTAS2R39, but did not give sufficient insight into understanding of the general molecular signature involved in bitter receptor activation of (iso)flavonoids. Therefore, 3D modeling was used as a next step in understanding which chemical characteristics influence bitter receptor interaction.

3D-Pharmacophore Modeling. The structural requirements for (iso)flavonoids to activate hTAS2R14 were best described by a five-feature pharmacophore (Figure 5A), of which all five features had to be mapped. It comprised two hydrogen donor features, one hydrogen acceptor feature, one "hydrophobic aromatic" feature, and one "ring aromatic" feature. The ROC plot area under the curve value was 0.751 (for confusion matrices and ROC plots, see Supporting Information S11−S14). This model was able to correctly predict the activation or absence of activation of two-thirds of the ligands and performed better for highly active than for moderately active compounds (the division into threshold groups is shown in Table 2). Of the highly active compounds, 81% were predicted correctly, but for the moderately active compounds this was 52%. Two-thirds of the inactive compounds were predicted correctly. The reason behind and remedy for incorrect predictions will be discussed in another section.

The best results for modeling the activation of hTAS2R39 by (iso)flavonoids were achieved with a six-feature pharmacophore (shown in Figure 5B), which allowed the ligands to map five of six features. It comprised three hydrogen donor features, one hydrogen acceptor feature, one "hydrophobic aromatic" feature, and one "ring aromatic" feature. The ROC plot area under the curve value was 0.873 while returning nine false positives and three false negatives. This model was able to map 84% of the compounds correctly. Divided into threshold groups, 94% of

Table 2. Classification of Ligands into Threshold Groups Highly Active (≤32 μM), Moderately Active (>32−500 μM), and Inactive (Not Active up to 500 μM)[a]

	hTAS2R14					hTAS2R39				
		true		false			true		false	
activity	total	+	−	+	−	total	+	−	+	−
high	27	22	−	−	5	35	33	−	−	2
moderate	23	12	−	−	11	28	21	−	−	7
inactive	23	−	15	8	−	14	−	11	3	−

[a]For 3D-pharmacophore modeling, the number of ligands per threshold group is given for hTAS2R14 and hTAS2R39 and subdivided by their model prediction into true/false positives/negatives. Several compounds measured were not included in the modeling.

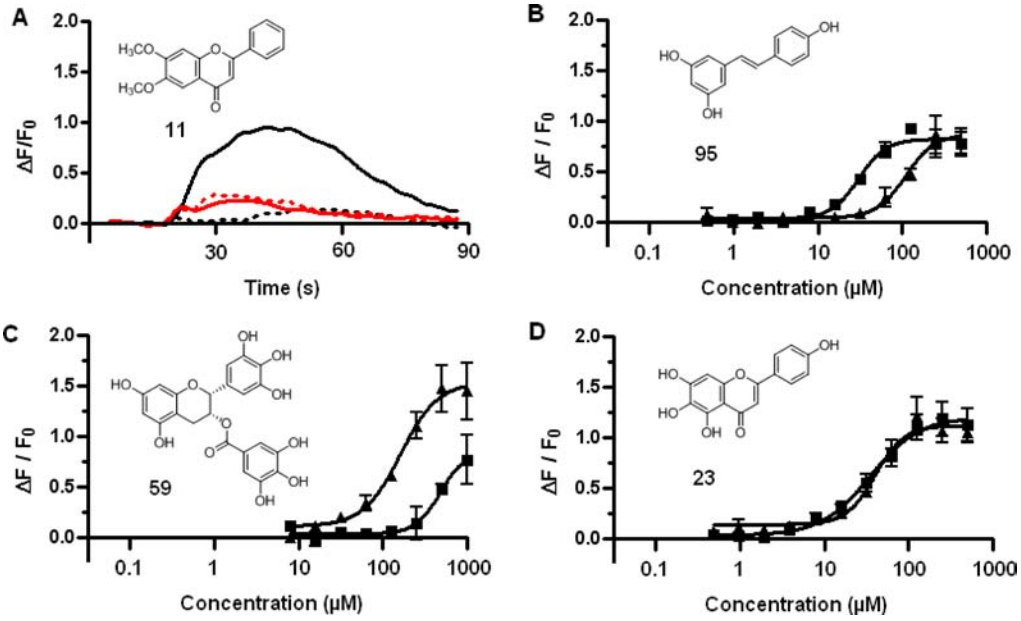

Figure 1. Effect of 500 μM 6,7-dimethoxyflavone (**11**) on hTAS2R14 (solid black line) and hTAS2R39 (solid red line) and on the corresponding noninduced cells, not expressing the bitter receptors (dashed black line) and (dashed red line) (A); dose−response curves of resveratrol (**95**) (B), epigallocatechin gallate (**59**) (C), and scutellarein (**23**) (D) on both bitter receptors hTAS2R14 (■) and hTAS2R39 (▲).

the highly active compounds, 75% of the moderately active compounds, and 79% of the inactive compounds were predicted correctly.

Visualization of Mapped Molecules. In Figure 6A, the pharmacophore for hTAS2R14 ligands is shown including the mapped molecule luteolin (**20**). The features of the pharmacophore almost precisely mapped the respective atoms of the flavonoid. This was reflected in an excellent fit value of 4.9, very close to the maximal attainable fit value of 5. The molecule was mapped with a relative energy of 0.14 kcal/mol, meaning that it required little energy to fit the conformation of the molecule into the pharmacophore. Compound **78** (7,4′-dimethoxy-5-hydroxyisoflavone) was unable to activate hTAS2R14, which is illustrated by suboptimal mapping (Figure 6B). One hydrogen bond donor feature did not map at all, which is indicated by a darker shade of pink in this feature than when the feature mapped. The structure of 7,4′-dimethoxy-5-hydroxyisoflavone (**78**) was applied with the relative energy 6.4 kcal/mol. So even with rotation, translation, and torsion, and despite a reasonable fit value of 2.1, the molecule did not map, in accordance with the compound being inactive. Often, high fit values indicate good mapping, but low fit values do not necessarily mean mismapping of molecules. As long as all features are met somehow, a bad fit value can still lead to activation. This is, for example, the case for 7,8,4′-trihydroxyisoflavone (**91**), which has a fit value of 0.8, but still maps the features and activates the receptor.

In Figure 6C, kaempferol (**35**) is mapped on the pharmacophore for hTAS2R39. The points in the middle of the sphere and the position of the respective atoms were close to each other. The mapping of the ligand was good, which is reflected in a fit value of 5.0 (of 6 maximum attainable). Figure 6D shows an inactive flavonoid on hTAS2R39, namely, 4′-hydroxy-6-methoxyflavone (**18**). As shown by the darker shade of pink, two of the three hydrogen donor features did not map at all.

To illustrate the influence of the absence of a C-ring, the mapped molecules for a chalcone (butein (**60**)) and a stilbene (resveratrol (**95**)) are depicted in Figure 6, panels E and F, respectively. As a result of the flexibility of butein (**60**), it mapped most of the features of the hTAS2R39 very well, except for the shifted hydrogen bond acceptor feature, resulting in a good fit value of 4.8. Its relative energy used for modeling was very low (0.08 kcal/mol).

Although the aromatic rings of resveratrol (**95**) are in closer proximity to each other than in flavonoids, it mapped the hTAS2R14 pharmacophore with all five features (fit value = 3.6, relative energy = 0.06 kcal/mol), indicating that the pharmacophore model might also be applicable to compounds that are structurally similar to flavonoids. Thus, a small variation

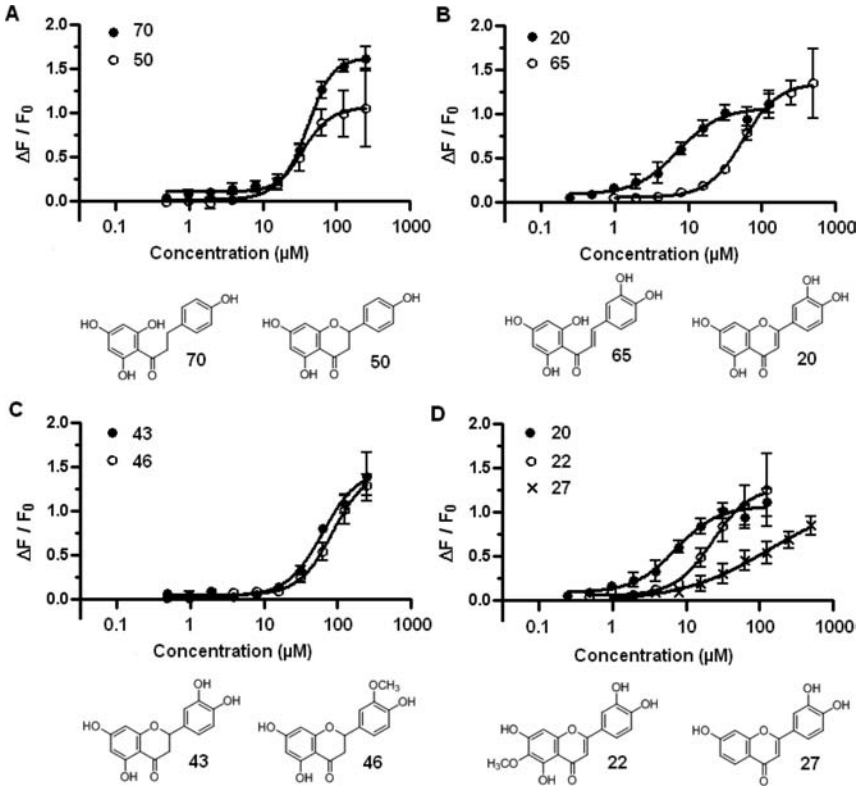

Figure 2. Comparison of dose−response curves on hTAS2R39 of phloretin (**50**) and naringenin (**70**) (A), luteolin (**20**) and eriodictyolchalcone (**65**) (B), eriodictyol (**43**) and homoeriodictyol (**46**) (C), and 3′,4′,7-trihydroxyflavone (**27**), 6-methoxyluteolin (**22**), and luteolin (**20**) (D).

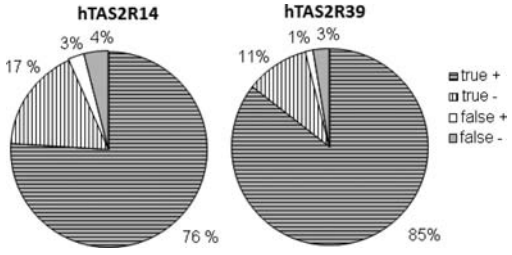

Figure 3. Predictions of 2D-fingerprint models with true positives, true negatives, false positives, and false negatives (in percentage) for hTAS2R14 (n = 75) and hTAS2R39 (n = 76) ligands.

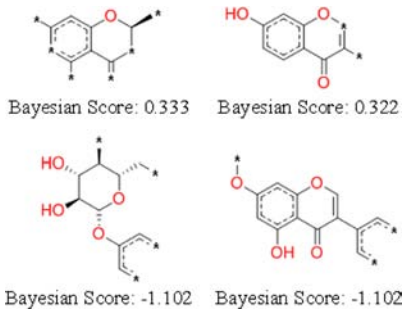

Figure 4. Selected "good" (positive Bayesian score) and "bad" (negative Bayesian score) fingerprint fragments for hTAS2R14.

in distance might have a minor influence on binding. This is not self-evident, as the length of a molecule can be crucial for receptor activation, which can be observed for estrogen receptor agonists.[30]

Furthermore, the C-ring seems to be of less influence for bitter receptor activation than the A- and B-rings. This is coherent with the observations in our previous study on isoflavonoids,[7] showing that the hydroxylation positions on A- and B-rings were more crucial for activation than the exact structure in the center (e.g., C-ring) of the molecule.

DISCUSSION

(Iso)flavonoid Agonists of hTAS2R14 and hTAS2R39 and Their Effects on Bitter Taste Receptors and Taste Perception. Among aglycones, catechins are the most important group of flavonoids occurring in our diet. We identified catechins as agonists of two bitter receptors, hTAS2R14 and hTAS2R39. Previously, only activation of hTAS2R39 was reported.[14] On hTAS2R39, we identified thresholds of ECG, EGCG, EC, and EGC to be 32, 32, 250, and 500 μM, respectively. Previously reported thresholds were between 10 and 30 μM for all four catechins.[14] Thus, our thresholds for galloylated catechins were in the same range as the previously reported thresholds, but we observed by a factor of 10 higher thresholds for the nongalloylated catechins. The same trend applied to the observed EC_{50} values on hTAS2R39. We obtained EC_{50} values of 150.6 and 161.2 μM for ECG and EGCG, respectively, and values for EC and EGC could not be calculated within the suitable concentration range (EC_{50} values reported by Narukawa[14] for ECG, EGCG, EGC, and EC were 88.2, 181.6, 395.5, and 417.7 μM, respectively). In another recent publication,[16] EC was identified as an agonist for three bitter receptors: hTAS2R39 (threshold = 1 mM, EC_{50} = 3.8 mM), hTAS2R4 (threshold = 2 mM, EC_{50} = 30.2 mM), and hTAS2R5 (threshold = 1 mM, EC_{50} = 3.2 mM). We additionally identified hTAS2R14 (threshold = 500 μM; no EC_{50} determined). Thus, differences are reported between the various bitter receptor assays, which might be caused by

dx.doi.org/10.1021/jf403387p | J. Agric. Food Chem. 2013, 61, 10454−10466

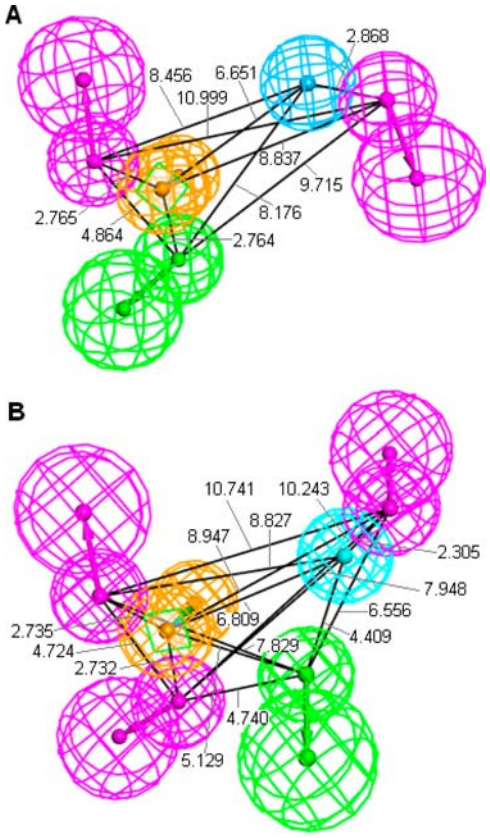

Figure 5. Pharmacophores for hTAS2R14 (A) and hTAS2R39 (B). The colors of the spheres represent the following features: pink, hydrogen donors; green, hydrogen acceptors; blue, hydrophobic aromatic; and yellow, ring aromatic. The green rectangle represents a plane within a ring structure. The small spheres indicate the presence of the feature on the ligand, and the large spheres indicate the possible position of the amino acids on the receptor, interacting with this feature. The direction of interaction is shown with an arrow. The numbers represent the distance between the features in ångströms.

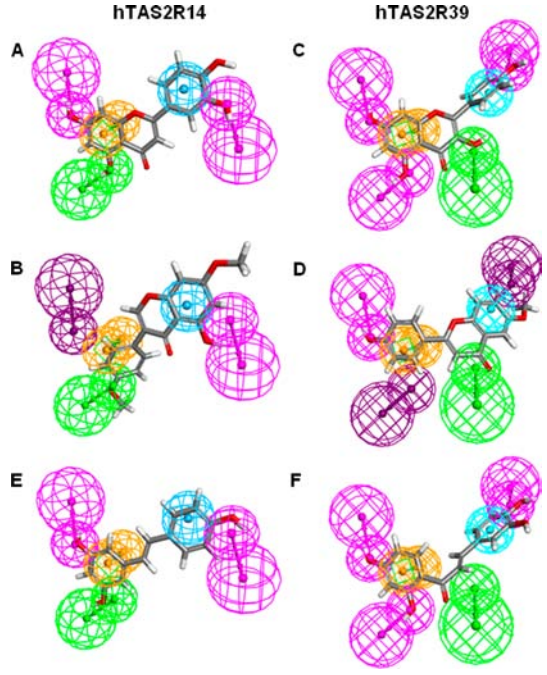

Figure 6. Examples of hTAS2R14 ligand pharmacophores including luteolin (**20**) (A), 7,4′-dimethoxy-5-hydroxyisoflavone (**78**) (B), and resveratrol (**95**) (E); examples of hTAS2R39 ligand pharmacophores including kaempferol (**35**) (C), 4′-hydroxy-6-methoxyflavone (**18**) (D), and butein (**60**) (F).

differences in experimental conditions. It should also be noted that in vitro threshold values reported in the elevated micromolar or in the millimolar range are very high, and, for example, in the case of EC in green tea, are unlikely to contribute to the bitter taste of the product.

Among the many new agonists of hTAS2R14 and hTAS2R39 reported in this study, some compounds were known as bitter before (e.g., taxifolin, resveratrol), some compounds had unknown taste properties (e.g., synthetic flavonoids), and three compounds were previously reported as bitter taste maskers (homoeriodictyol, eriodictyol, and phloretin[22,31]). We identified homoeriodictyol and eriodictyol as agonists of hTAS2R14 (thresholds of 32 μM for both compounds) and hTAS2R39 (thresholds of 32 and 16 μM, respectively). These two compounds were reported to mask the bitterness of caffeine in sensory tests without exhibiting strong taste characteristics at 100 ppm.[31] The molecular mechanism of masking by homoeriodictyol and eriodictyol requires further clarification. For phloretin, it was reported that its masking activity (50 mg/L (= 182 μM)) for caffeine in sensory tests competed with its bitterness observed at elevated concentrations (100 mg/L (= 365 μM)).[22] It was suggested that this might be an overlapping effect of antagonistic and agonistic activities, as described for sesquiterpene lactones.[32] We identified phloretin as agonists of hTAS2R14 and hTAS2R39 (thresholds of 16 and 8 μM, respectively). Thus, the bitterness of phloretin could be caused by activation of hTAS2R14 and hTAS2R39 and possibly other receptors. Remarkably, the bitterness threshold of phloretin in vivo was ∼20−40-fold higher than in vitro. It has been observed before[10] that bitter compounds (hop acids) can display higher sensory than receptor thresholds. In the case of hop acids, this has been ascribed to their interaction with the oral mucosa. A bitter receptor assay might thus overestimate bitterness, as interaction with mucosa or other in vivo conditions is not accounted for. Nevertheless, overestimation is not necessarily the case, as similar in vivo and in vitro thresholds have been reported for β-D-glucopyranosides[33] and tea catechins.[14]

Evaluation of the 2D and 3D Models. Even though they operated with only planar compound structures, the 2D-fingerprint models were very effective in predicting active compounds and discriminating them from inactive compounds, leading to low numbers of false predictions. This might be due to the relatively planar nature of many (iso)flavonoids. The 2D-fingerprint models can be used as a quick in silico screening tool in compound library screening to identify (iso)flavonoid (or similar) compounds that might taste bitter. Due to lower complexity, they are more suitable than the 3D-pharmacophore models for screening large compound databases. On the contrary, 2D-fingerprint models created only a partial understanding of the molecular features involved in bitter receptor activation. The 3D-pharmacophore models provided a broader insight into (iso)flavonoid bitter receptor interaction. The structural characteristics for an (iso)flavonoid to activate hTAS2R14 (or hTAS2R39) were determined to be composed of two (or three) hydrogen bond donor sites, one hydrogen bond acceptor site, one hydrophobic ring structure, and one aromatic ring structure.

The receptor activation threshold values lie within a range of 3 orders of magnitude, which is generally considered as a relatively small range for quantitative structure−activity relationship (QSAR) modeling. In the attempt to establish a QSAR model, a clear correlation between features and threshold could not be determined, but even without a quantitative prediction, the pharmacophore models are a powerful tool in the prediction of potential bitterness.

Explanation of False Predictions by 3D-Pharmacophore Models. Several compounds were falsely predicted as positive or negative by the 3D-pharmacophore models (see Table 2).

The highly active false negatives, that is, the actives from the cell assay that did not map to the pharmacophores, had a lack of substituents on the B-ring of the (iso)flavonoid in common. In most cases, as shown in Figure 7A for pinocembrin (**51**), the donor feature next to the hydrophobic aromatic feature in the pharmacophore for hTAS2R14 ligands could not be mapped by these molecules. Consequently, the model classified these molecules as inactive. The pharmacophore model for hTAS2R39 ligands was able to recognize more of these unsubstituted ligands, probably due to the mapping setting, which allowed the ligands to miss one feature. The question arises whether the donor feature next to the hydrophobic aromatic group might be irrelevant or of less importance for binding. Another explanation could be that a second mode of binding to the receptor for ligands without substitution on the B-ring occurs. Thus, the current pharmacophore models are limited to (iso)flavonoids that contain two (for hTAS2R14) or at least one (for hTAS2R39) substituted aromatic ring(s). Nevertheless, naturally occurring (iso)flavonoids are mostly substituted (exceptions are, e.g., pinocembrin and chrysin) and therefore applicable to the model.

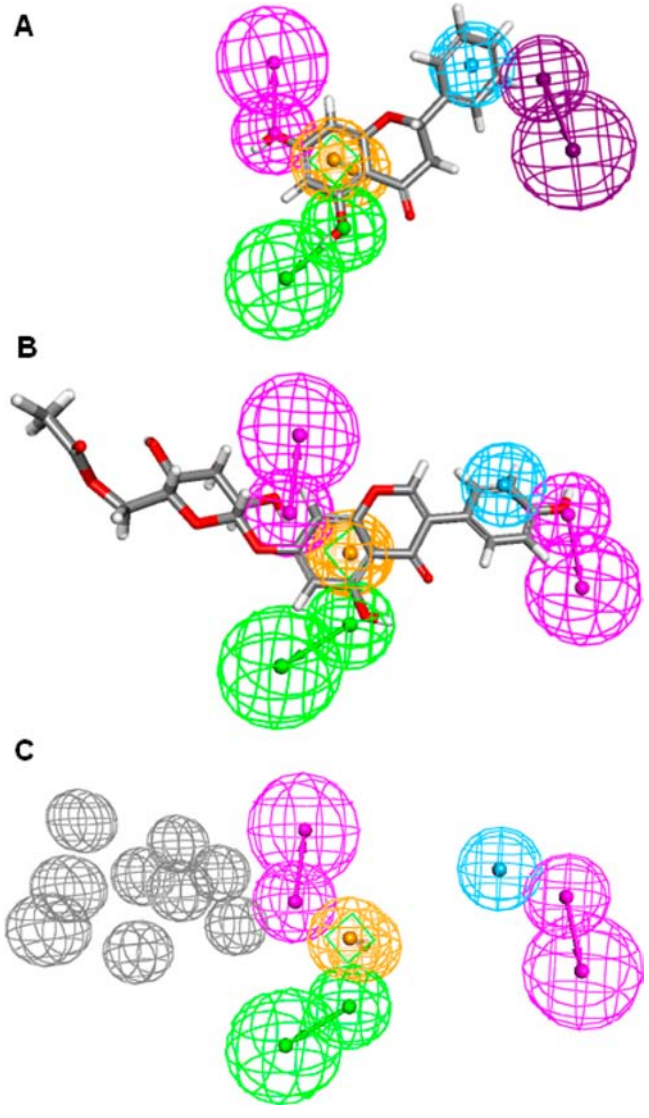

Figure 7. Falsely negative predicted compound pinocembrin (**51**) on the hTAS2R14 ligand pharmacophore (A); falsely positive predicted compound acetylgenistin (**74**) on the hTAS2R14 ligand pharmacophore (B); excluded volumes on the hTAS2R14 ligand pharmacophore (C).

False positives, that is, molecules which mapped to the pharmacophore(s), even though they did not activate the receptor(s), were obtained as well. Only three compounds were falsely predicted as positive for hTAS2R39 and eight compounds for hTAS2R14. Of these eight, five were isoflavones glucosylated on position 7 of the A-ring (example given for **74** in Figure 7B), which might cause steric hindrance for optimal receptor binding. To prevent these false positive predictions, excluded volumes might be added to the pharmacophore model for receptor hTAS2R14, as shown in Figure 7C. However, this option should be used only for isoflavones, as structures with other backbones have not been tested. Furthermore, because only the glucoside substitutions on position 7 typical for isoflavones were tested, no statement can be made about other glycosylation positions frequently occurring in flavonoids, such as position 3. Thus, the resulting model for hTAS2R14 ligands is limited to aglycones, whereas the model for hTAS2R39 ligands can be used for certain glycosides as well. An additional reason for false positive prediction might be a solubility issue. Some compounds (for example, **1** and **14**) had limited solubility at high concentrations; thus, their real potential to act as bitter compounds might have been underestimated.

In conclusion, the prediction of the generated pharmacophore models for activation of receptors hTAS2R14 and hTAS2R39 by (iso)flavonoids was successful, and most false positive and false negative predictions could be explained, leading to an understanding of 88% of hTAS2R14 ligands and 94% of hTAS2R39 ligands within this study. The combination of in vitro and in silico data created a good insight into activation of hTAS2R14 and hTAS2R39 by (iso)flavonoids.

Comparison of Ligand-Based Pharmacophore Models for hTAS2R14 and hTAS2R39. The difference between the two pharmacophore models indicated that despite the largely overlapping ligands of both receptors, there was a difference in the molecular structure and substitution pattern of ligands recognized by receptors hTAS2R14 and hTAS2R39. The additional donor feature of the pharmacophore model for hTAS2R39 ligands indicated the possible presence of another complementary acceptor site in the binding pocket of hTAS2R39 compared to hTAS2R14. This might explain why the OH-rich compounds showed different behaviors on the two bitter receptors, as can be observed for compounds **24**, **32**, and **58**, which activate only hTAS2R39, but not hTAS2R14, and for compounds **38**, **39**, **57**, and **59**, which have a much higher activity on hTAS2R39 than on hTAS2R14. Another explanation might be that the hydrophobic aromatic feature, and therewith hydrophobic interaction with the binding site, is of

higher importance in hTAS2R14 than in hTAS2R39, as compounds with three OH groups on the B-ring (**24**, **38**, **58**, and **59**) have a decreased hydrophobicity on this aromatic ring and no or decreased activity on hTAS2R14.

Both pharmacophore models have two donor features, which seem to be equally relevant for discrimination between the active and inactive ligands. The aromatic features and the acceptor feature did not seem to have a strong discriminator function, but they might play a role in ligand alignment.

Tuning Breadth of Bitter Taste Receptors. To date, hTAS2R14 has been regarded as a more broadly tuned receptor, compared to hTAS2R39.[9] This idea was based on the activation of hTAS2R14 by structurally very diverse compounds and the fact that fewer agonists for hTAS2R39 were known. During recent years, numerous new agonists have been reported for hTAS2R39,[7,14,15,17] including the large number of flavonoids from the present study, which exceeds the number of hTAS2R39 agonists known before. Hence, hTAS2R39 is revealed to be activated by many more agonists than initially thought. Also, the number of hTAS2R14 agonists keeps increasing (refs 7 and 13 and this study).

With time, the number of hTAS2R agonists will grow further, and it is questionable whether tuning breadth should simply be related to the number of bitter receptor agonists. Our present results show that the substitution pattern of (iso)flavonoids was of higher importance for receptor activation than their backbone structure (e.g., whether the agonist is a flavone or a flavanone). Our pharmacophore modeling revealed which signatures underlay binding to hTAS2R14 and hTAS2R39. Therefore, it might be better to describe tuning breadth of bitter receptors in terms of the number of molecular signatures recognized by the receptor. In this way, a collection of molecules with similar signatures will count only as one with respect to tuning breadth, and tuning breadth is less likely to be overestimated.

In conclusion, this study identified many flavonoids as intrinsically bitter and elucidated the structural requirements for bitterness of (iso)flavonoids. Understanding their "bitter motif" might prevent the introduction of bitter taste in the design of functional foods enriched in (iso)flavonoid bioactives.

■ ASSOCIATED CONTENT

Ⓢ Supporting Information

SMILES of tested compounds and additional information on 2D-fingerprint modeling and 3D-pharmacophore modeling. This material is available free of charge via the Internet at http://pubs.acs.org. The pharmacophore models are available upon request to the corresponding author. The newly identified bitter receptor ligands will be uploaded into BitterDB (http://bitterdb.agri.huji.ac.il/bitterdb/),[34] a free and searchable database of bitter compounds and bitter receptors.

■ AUTHOR INFORMATION

Corresponding Author

*(J.-P. V.) Mailing address: Wageningen University, Laboratory of Food Chemistry, Bornse Weilanden 9, 6708 WG Wageningen, The Netherlands. Phone: +31 317 482888. E-mail: jean-paul.vincken@wur.nl.

Present Address

#(G.S.) Valio Ltd. R&D, 00370 Helsinki, Finland.

Funding

This work was financially supported by the Food and Nutrition Delta of the Ministry of Economic Affairs, The Netherlands (FND 08019).

Notes

The authors declare no competing financial interest.

■ ACKNOWLEDGMENTS

We thank Dr. Michiel Gribnau (Unilever Vlaardingen, The Netherlands) for statistical analysis and Diana Drennan (Unilever Trumbull, CT, USA, currently employed at Accelrys, USA) and Katalin Nedassy (Accelrys, UK) for advice in modeling.

■ REFERENCES

(1) Setchell, K. D. R.; Cassidy, A. Dietary isoflavones: biological effects and relevance to human health. *J. Nutr.* **1999**, *129* (3), 758S−767S.

(2) Manach, C.; Scalbert, A.; Morand, C.; Rémésy, C.; Jiménez, L. Polyphenols: food sources and bioavailability. *Am. J. Clin. Nutr.* **2004**, *79* (5), 727−747.

(3) Soto-Vaca, A.; Gutierrez, A.; Losso, J. N.; Xu, Z.; Finley, J. W. Evolution of phenolic compounds from color and flavor problems to health benefits. *J. Agric. Food Chem.* **2012**, *60* (27), 6658−6677.

(4) Drewnowski, A.; Gomez-Carneros, C. Bitter taste, phytonutrients, and the consumer: a review. *Am. J. Clin. Nutr.* **2000**, *72* (6), 1424−1435.

(5) Aldin, E.; Reitmeier, C. A.; Murphy, P. Bitterness of soy extracts containing isoflavones and saponins. *J. Food Sci.* **2006**, *71* (3), S211−S215.

(6) Okubo, K.; Iijima, M.; Kobayashi, Y.; Yoshokoshi, M.; Uchida, T.; Kudou, S. Components responsible for the undesirable taste of soybean seeds. *Biosci., Biotechnol., Biochem.* **1992**, *56* (1), 99−103.

(7) Roland, W. S. U.; Vincken, J. P.; Gouka, R. J.; van Buren, L.; Gruppen, H.; Smit, G. Soy isoflavones and other isoflavonoids activate the human bitter taste receptors hTAS2R14 and hTAS2R39. *J. Agric. Food Chem.* **2011**, *59* (21), 11764−11771.

(8) Behrens, M.; Brockhoff, A.; Kuhn, C.; Bufe, B.; Winnig, M.; Meyerhof, W. The human taste receptor hTAS2R14 responds to a variety of different bitter compounds. *Biochem. Biophys. Res. Commun.* **2004**, *319* (2), 479−485.

(9) Meyerhof, W.; Batram, C.; Kuhn, C.; Brockhoff, A.; Chudoba, E.; Bufe, B.; Appendino, G.; Behrens, M. The molecular receptive ranges of human TAS2R bitter taste receptors. *Chem. Senses* **2010**, *35* (2), 157−170.

(10) Intelmann, D.; Batram, C.; Kuhn, C.; Haseleu, G.; Meyerhof, W.; Hofmann, T. Three TAS2R bitter taste receptors mediate the psychophysical responses to bitter compounds of hops (*Humulus lupulus* L.) and beer. *Chemosens. Percept.* **2009**, *2* (3), 118−132.

(11) Le Neve, B.; Foltz, M.; Daniel, H.; Gouka, R. The steroid glycoside H.g.-12 from *Hoodia gordonii* activates the human bitter receptor TAS2R14 and induces CCK release from HuTu-80 cells. *Am. J. Physiol.-Gastrointest. Liver Physiol.* **2010**, *299* (6), G1368−G1375.

(12) Maehashi, K.; Matano, M.; Wang, H.; Vo, L. A.; Yamamoto, Y.; Huang, L. Bitter peptides activate hTAS2Rs, the human bitter receptors. *Biochem. Biophys. Res. Commun.* **2008**, *365* (4), 851−855.

(13) Hellfritsch, C.; Brockhoff, A.; Stähler, F.; Meyerhof, W.; Hofmann, T. Human psychometric and taste receptor responses to steviol glycosides. *J. Agric. Food Chem.* **2012**, *60* (27), 6782−6793.

(14) Narukawa, M.; Noga, C.; Ueno, Y.; Sato, T.; Misaka, T.; Watanabe, T. Evaluation of the bitterness of green tea catechins by a cell-based assay with the human bitter taste receptor hTAS2R39. *Biochem. Biophys. Res. Commun.* **2011**, *405* (4), 620−625.

(15) Ueno, Y.; Sakurai, T.; Okada, S.; Abe, K.; Misaka, T. Human bitter taste receptors hTAS2R8 and hTAS2R39 with differential functions to recognize bitter peptides. *Biosci., Biotechnol., Biochem.* **2011**, *75* (6), 1188−1190.

(16) Soares, S.; Kohl, S.; Thalmann, S.; Mateus, N.; Meyerhof, W.; De Freitas, V. Different phenolic compounds activate distinct human bitter taste receptors. *J. Agric. Food Chem.* **2013**, *61* (7), 1525−1533.
(17) Kohl, S.; Behrens, M.; Dunkel, A.; Hofmann, T.; Meyerhof, W. Amino acids and peptides activate at least five members of the human bitter taste receptor family. *J. Agric. Food Chem.* **2013**, *61* (1), 53−60.
(18) Martinez-Mayorga, K.; Medina-Franco, J. L. Chemoinformatics − applications in food chemistry. In *Advances in Food and Nutrition Research*, 58th ed.; Academic Press: Burlington, MA, 2009; pp 33−56.
(19) Glen, R. C.; Bender, A.; Arnby, C. H.; Carlsson, L.; Boyer, S.; Smith, J. Circular fingerprints: flexible molecular descriptors with applications from physical chemistry to ADME. *IDrugs* **2006**, *9* (3), 199−204.
(20) Wermuth, C. G.; Ganellin, C. R.; Lindberg, P.; Mitscher, L. A. Glossary of terms used in medicinal chemistry (IUPAC Recommendations 1998). *Pure Appl. Chem.* **1998**, *70* (5), 1129−1143.
(21) Van Drie, J. H. Monty Kier and the origin of the pharmacophore concept. *Internet Electron. J. Mol. Des.* **2007**, *6* (9), 271−279.
(22) Ley, J. P.; Dessoy, M.; Paetz, S.; Blings, M.; Hoffmann-Lücke, P.; Reichelt, K. V.; Krammer, G. E.; Pienkny, S.; Brandt, W.; Wessjohann, L. Identification of enterodiol as a masker for caffeine bitterness by using a pharmacophore model based on structural analogues of homoeriodictyol. *J. Agric. Food Chem.* **2012**, *60* (25), 6303−6311.
(23) Kraft, P.; Bajgrowicz, J. A.; Denis, C.; Fráter, G. Odds and trends: recent developments in the chemistry of odorants. *Angew. Chem.−Int. Ed.* **2000**, *39* (17), 2981−3010.
(24) Tromelin, A.; Guichard, E. Use of catalyst in a 3D-QSAR study of the interactions between flavor compounds and β-lactoglobulin. *J. Agric. Food Chem.* **2003**, *51* (7), 1977−1983.
(25) Chandrashekar, J.; Mueller, K. L.; Hoon, M. A.; Adler, E.; Feng, L.; Guo, W.; Zuker, C. S.; Ryba, N. J. P. T2Rs function as bitter taste receptors. *Cell* **2000**, *100* (6), 703−711.
(26) Kuhn, C.; Bufe, B.; Winnig, M.; Hofmann, T.; Frank, O.; Behrens, M.; Lewtschenko, T.; Slack, J. P.; Ward, C. D.; Meyerhof, W. Bitter taste receptors for saccharin and acesulfame K. *J. Neurosci.* **2004**, *24* (45), 10260−10265.
(27) Hawkins, D. M.; Basak, S. C.; Mills, D. Assessing model fit by cross-validation. *J. Chem. Inf. Comput. Sci.* **2003**, *43* (2), 579−586.
(28) Clifford, M. N. Anthocyanins − nature, occurrence and dietary burden. *J. Sci. Food Agric.* **2000**, *80* (7), 1063−1072.
(29) Awika, J. M. Behavior of 3-deoxyanthocyanidins in the presence of phenolic copigments. *Food Res. Int.* **2008**, *41* (5), 532−538.
(30) Fang, H.; Tong, W.; Perkins, R.; Soto, A. M.; Prechtl, N. V.; Sheehan, D. M. Quantitative comparisons of in vitro assays for estrogenic activities. *Environ. Health Perspect.* **2000**, *108* (8), 723−729.
(31) Ley, J. P.; Krammer, G.; Reinders, G.; Gatfield, I. L.; Bertram, H. J. Evaluation of bitter masking flavanones from Herba Santa (*Eriodictyon californicum* (H. & A.) Torr., Hydrophyllaceae). *J. Agric. Food Chem.* **2005**, *53* (15), 6061−6066.
(32) Brockhoff, A.; Behrens, M.; Roudnitzky, N.; Appendino, G.; Avonto, C.; Meyerhof, W. Receptor agonism and antagonism of dietary bitter compounds. *J. Neurosci.* **2011**, *31* (41), 14775−14872.
(33) Bufe, B.; Hofmann, T.; Krautwurst, D.; Raguse, J. D.; Meyerhof, W. The human TAS2R16 receptor mediates bitter taste in response to β-glucopyranosides. *Nat. Genetics* **2002**, *32* (3), 397−401.
(34) Wiener, A.; Shudler, M.; Levit, A.; Niv, M. Y. BitterDB: a database of bitter compounds. *Nucleic Acids Res.* **2012**, *40* (D1), D413−D419.